Long-term study on the physical characteristics of polar aerosols at the King Sejong Station, Antarctic Peninsula

J. Kim[1,*], Y.J. Yoon[1,**], Y. Gim[1], H.J. Kang[1], J.H. Choi[1], and B.Y. Lee[1]
[1]Korea Polar Research Institute, Incheon, 21990, Republic of Korea
* Presentation author: J. Kim (jaeseok.kim@kopri.re.kr) **Corresponding author: Y.J. Yoon (yjyoon@kopri.re.kr)

Introduction

The Antarctic region is highly sensitive to climate changes due to complex interconnected environmental systems (e.g. snow cover, land ice, sea-ice, and ocean circulation) (Chen et al., 2009). Previous studies show that the Antarctic Continent and the Antarctic Peninsula have experienced noticeable climate changes (Steig et al., 2009; Pritchard et al., 2012; Schneider et al., 2012). The Antarctic Peninsula, in particular, has a warming rate of more than 5 times that of the other regions on earth (Vaughan et al., 2003; IPCC, 2013). The Antarctic climate system can be linked with aerosol particles by complex feedback processes that involve aerosol-cloud interactions. Although various studies have been performed to understand properties of aerosol particles, the measurements taken at the Antarctic Peninsula and the long-term observations of aerosol particles are still insufficient. In this study, we continuously monitored the physical characteristics of aerosol particles at the Korean Antarctic station (King Sejong Station) in the Antarctic Peninsula from March 2009. The main aim of this study is to determine the seasonal variations of the physical properties of aerosol particles in the Antarctic Peninsula.

Methods

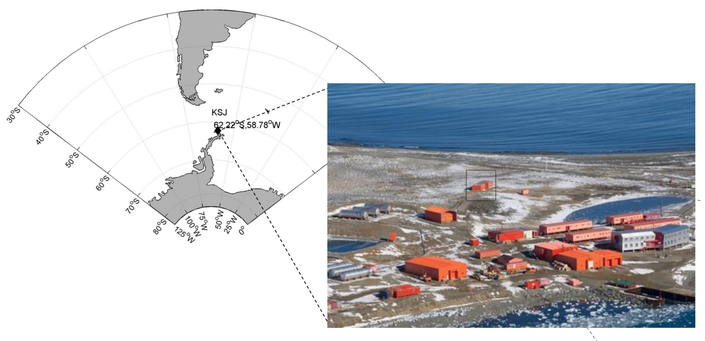

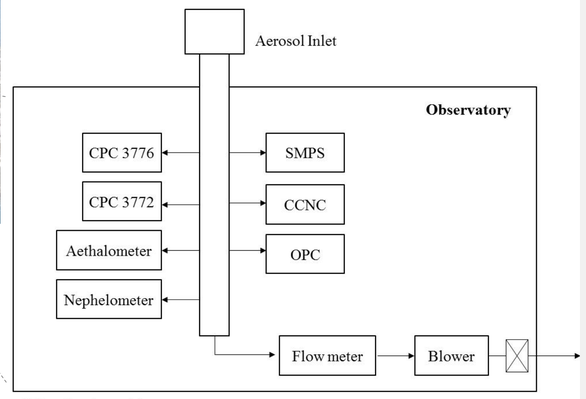

- Sampling site: King Sejong Station (62.22°S, 58.78°W)
- Sampling periods: Mar. 2009 – Feb. 2015
- Pollution sector: Northeastern direction (355°-55°)

Figure 1. Map of the sampling site and a schematic diagram for the observation instruments used in this study

Results and Discussions

I. Seasonal variations of total particle number concentrations

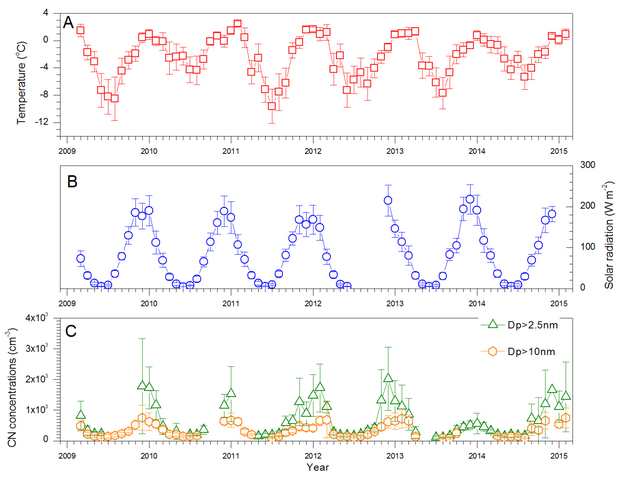

Figure 2. Monthly variation of mean values of (a) temperature, (b) solar radiation, and (c) CN concentrations of particles larger than 2.5 nm (green opened triangle) and 10 nm (yellow opened circle).

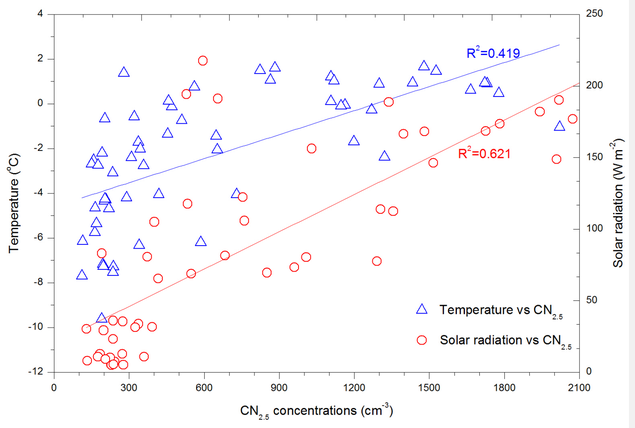

Figure 3. Relationship between monthly mean CN2.5 concentrations and monthly mean temperature (blue opened triangle) or monthly mean solar radiation intensity (red opened circle). Blue and red solid lines are a regression lines.

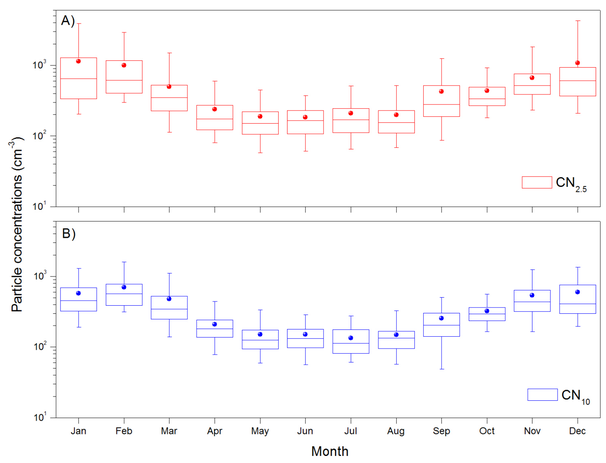

Figure 4. Box plots of seasonality of (a) $CN_{2.5}$ and (b) CN_{10} concentrations. Lines in the middle of the boxes indicate sample medians (mean: circle), lower and upper lines of the boxes are the 25th and 75th percentiles, and whiskers indicate the 5th and 95th percentiles.

II. Seasonality of CCN concentrations

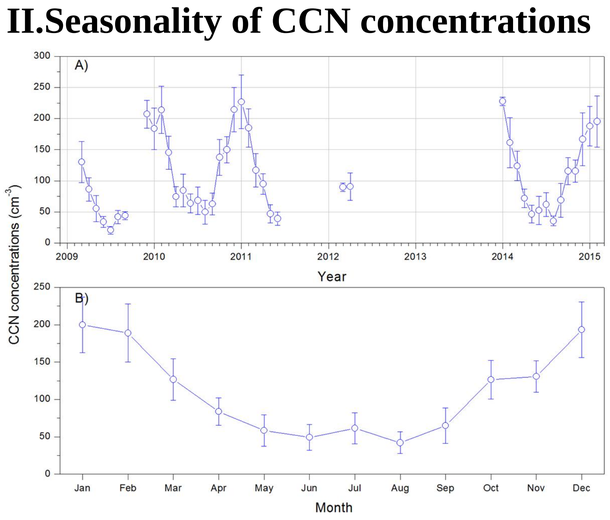

Figure 5. (a) Monthly mean CCN concentrations at the SS of 0.4 % with a standard deviation from March 2009 to February 2015 (b) Seasonal variation of mean CCN concentrations at the SS of 0.4 % with a standard deviation.

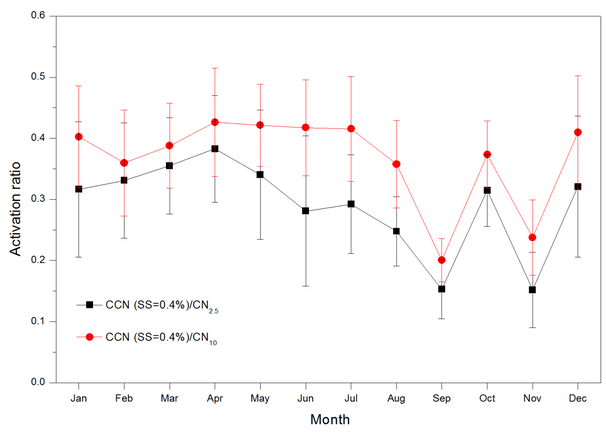

Figure 6. Comparison of the seasonal mean variation of the activation ratio between measurements (CPC 3776 and CPC 3772) by two CPCs.

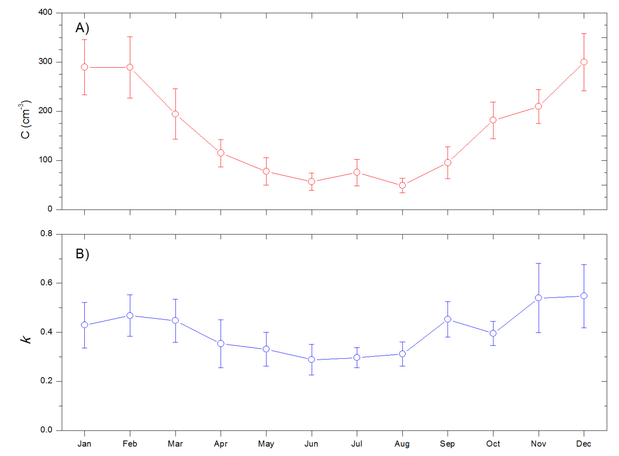

Figure 7. Seasonality of monthly mean values of (a) *C* and (b) *k* over the whole observation periods.

The power-law function,

$$N_{CCN} = C \times (SS)^k$$

where, N_{CCN} is the concentration of CCN at given a supersaturation values (SS), *C* and *k* are coefficient constants estimated from CCN spectra.

III. Effect origin and pathway of air mass

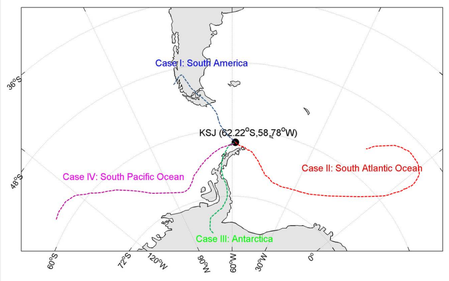

Figure 8. Classification of the four cases according to the origin and pathway of the air masses. Dot lines represent example of back trajectories according to cases.

Table 1. Summary of meteorology and aerosol data according to the origin and transport pathway of aerosol particles.

	Overall	Case I	Case II	Case III	Case IV
Wind speed (m/s)	8.4 ± 1.8	2.6 ± 1.1	6.0 ± 1.5	6.7 ± 1.7	8.6 ± 1.8
Wind direction (°)	237.2 ± 55.8	186.2 ± 20.7	155.9 ± 50.3	206.9 ± 52.3	242.7 ± 55.3
Black carbon concentration (ng/m³)	65.1 ± 29.2	122.2 ± 10.6	36.7 ± 14.2	65.6 ± 30.0	66.5 ± 29.5
CCN concentration (#/cm³)	129.7 ± 50.5	212.8 ± 50.2	146.0 ± 50.3	128.9 ± 34.9	128.7 ± 50.8
Particle concentration (Dp>2.5 nm) (#/cm³)	737.3 ± 849.4	374.9 ± 64.4	605.3 ± 517.6	578.9 ± 377.3	751.2 ± 877.1
Particle concentration (Dp>10 nm) (#/cm³)	347.8 ± 229.1	358.8 ± 61.2	268.8 ± 173.9	331.9 ± 133.0	352.2 ± 234.9
Frequency		3	113	118	2407

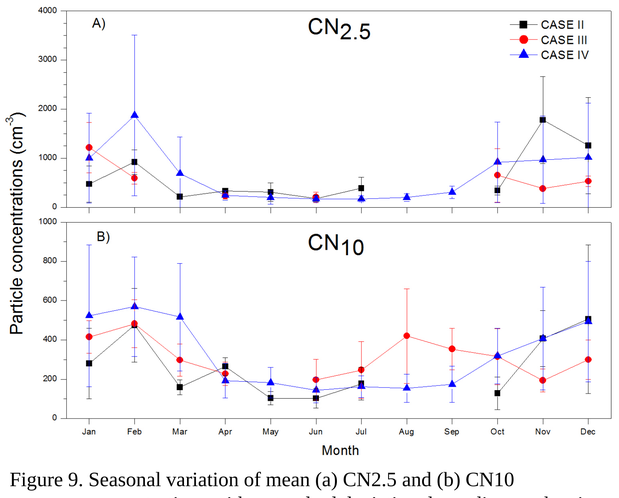

Figure 9. Seasonal variation of mean (a) CN2.5 and (b) CN10 concentrations with a standard deviation depending on the air mass origin.

Figure 10. Seasonal lognormally fitted size distribution of aerosol particles originating from the South Pacific Ocean, ranging from 0.01 to 0.3 μm (CASE IV).

Summary

- An obvious seasonal variation of CN and CCN concentrations exists, with the maximum concentrations in the austral summer (DJF) and the minimum concentrations in the winter (JJA).
- The activation ratio (CCN/CN_{10}) of aerosol particles at the King Sejong Station (0.40 ± 0.08) in the Antarctic Peninsula was lower than those at the Arctic sites (0.52), indicating that less hygroscopic compounds in aerosol particles should be dominant.
- The values of C varied between 6.35 cm^{-3} and 837.24 cm^{-3}, with a mean of 171.48 ± 62.00 cm^{-3}. The values of k ranged between 0.07 and 2.19, with a mean of 0.41 ± 0.10. The k values during austral the summer periods (DJF) were higher than those during the winter periods (JJA).
- The $CN_{2.5}$ concentrations that originated from oceanic areas (CASE II and IV) were higher than those from continental regions (CASE III), in particular, the $CN_{2.5}$ concentrations show clear seasonal variations; minimum concentrations from April to September and maximum concentrations in November from the South Atlantic Ocean (CASE II) and in February from the South Pacific Ocean (CASE IV).
- The modal diameter of aerosol particles that originated from the South Pacific Ocean (CASE IV) showed seasonal variations; 0.023 μm in the winter and 0.034 μm in the summer for the Aitken mode and 0.086 μm in the winter and 0.109 μm in the summer for the accumulation mode

References

- Chen, J. L., Wilson, C. R., Blankenship, D., and Tapley, B. D.: Accelerated Antarctic ice loss from satellite gravity measurements, Nat. Geosci., 2, 859-862, 10.1038/ngeo694, 2009.
- IPCC: Climate change 2013: The physical science basis, Intergovernmental panel on Climate Change, Cambridge University Press, New York, USA, 571-740, 2013.
- Pritchard, H. D., Ligtenberg, S. R. M., Fricker, H. A., Vaughan, D. G., Van Den Broeke, M. R., and Padman, L.: Antarctic ice-sheet loss driven by basal melting of ice shelves, Nature, 484, 502-505, 10.1038/nature10968, 2012.
- Schneider, D. P., Deser, C., and Okumura, Y.: An assessment and interpretation of the observed warming of West Antarctica in the austral spring, Clim. Dyn., 38, 323-347, 10.1007/s00382-010-0985-x, 2012.
- Steig, E. J., Schneider, D. P., Rutherford, S. D., Mann, M. E., Comiso, J. C., and Shindell, D. T.: Warming of the Antarctic ice-sheet surface since the 1957 International Geophysical Year, Nature, 457, 459-462, 10.1038/nature07669, 2009.
- Vaughan, D. G., Marshall, G. J., Connolley, W. M., Parkinson, C., Mulvaney, R., Hodgson, D. A., King, J. C., Pudsey, C. J., and Turner, J.: Recent rapid regional climate warming on the Antarctic Peninsula, Clim. Change, 60, 243-274, 10.1023/a:1026021217991, 2003.

Acknowledgements

We would like to thank the many technicians and scientists of the overwintering crews. This work was supported by a Korea Grant from the Korean Government (MSIP) (NRF-2016M1A5A1901769) (KOPRI-PN16081) and KOPRI project (PE16010).

Korea Polar Research Institute